

Original Research Articles

# Chitosan Decelerates Melanosis in Shrimp: A Novel Technique for Visual Quality Assessment Using Digital Image Analysis

Ali Eslam Kadak<sup>1a</sup><sup>1</sup> Fisheries Faculty, Kastamonu University

Keywords: Black spot, E-cognition, Definiens Developer, Waste recycling, Deep-water rose shrimp

<https://doi.org/10.46989/001c.88509>

---

## Israeli Journal of Aquaculture - Bamidgheh

Vol. 75, Issue 2, 2023

---

The study aimed to determine the effects of chitosan, sodium metabisulfite, and citric acid against melanosis, which causes significant economic losses during the storage of shrimps. For this purpose, two different types of chitosan were extracted from tiger prawn shell wastes. The extracted chitosan was characterized by viscosity, FT-IR, XRD, SEM imaging, and color analyses. Prevention of melanosis formation was investigated by testing chitosan, sodium metabisulfite, and citric acid. To achieve this, fresh deep-water pink shrimp samples immersed in different solutions were stored for 12 days at 4°C. Melanosis formation in the samples was observed via color measurement, sensory evaluation, and image analysis. According to the results of the research, the deacetylation degrees of chitosans were found to be 99.50 and 89.51% and 76.31 and 78.24% by two different methods, respectively. Viscosities were measured as 0.34 and 4.17 cSt, respectively. Regarding the color parameters, the L\* values were 83.68 and 78.94, a\* values were 0.55 and 2.71, and b\* values were 10.33 and 13.85, respectively. According to the sensory evaluation conducted throughout the study, melanosis formation was observed in all groups starting from the 6th day. On the 8th day, the control groups exceeded the acceptability threshold, and on the 12th day, melanosis formation spread throughout the body in all groups. The sensory evaluation results were supported by the color measurement and image analysis implemented for the first time in this study. The present study's results showed that chitosan obtained from shellfish wastes decelerates melanosis formation as an alternative to commercially used chemicals.

## INTRODUCTION

Shrimp is among the most important seafood due to its high nutritional and commercial value. The world shellfish production is around 11.2 million tons/year, the shrimp production accounting for more than 7 million tons/year.<sup>1</sup> In Türkiye, shrimp is caught from the Marmara, Aegean, and Mediterranean coasts. The amount of shrimp caught from these regions, of which a significant portion is exported after processing, is approximately 5500 tons/year.<sup>2</sup>

Shrimp is a highly perishable seafood. Its deterioration primarily originates from biological reactions, i.e., decomposition mediated by microbial or endogenous enzymes, protein degradation, or lipid oxidation. One of the most significant spoilage reasons for shrimp is the accumulation of undesired compounds from biochemical reactions and microbiological growth.<sup>3</sup>

The color change is among the most crucial quality problems of shrimp after capture. This color change is called

“melanosis,” “blackening,” or “black spot.” Tyrosine and hydroxyphenylalanine emerge due to the decomposition of the proteins in shrimp meat. These amino acids are oxidized and transformed into melanin pigments with the effect of the tyrosinase enzyme. The blackening is most commonly encountered around the head and legs due to excessive tyrosinase enzyme. The contribution of environmental factors (light, temperature, microbial, etc.) in the formation and development of melanosis is very significant. In addition, delayed decapitation and application of insufficient cooling or no cooling after capture accelerates the process. While the color change is only at appearance first, it later manifests itself in the meat, causing deterioration in quality and thus economic losses.<sup>4-6</sup> Shrimps are usually immersed in sodium metabisulfite solution to eliminate this damage and prevent color change. However, in addition to avoiding the color change in shrimps, this substance's residue amount must be at a level that does not threaten human health. The potential risks of sodium metabisul-

---

a a Corresponding Ali Eslam Kadak, alieslem@hotmail.com

fit in terms of human health necessitated strict control of its use, and many countries added this substance to the 'positive list', which shows the maximum concentration in foods, and republished it.<sup>7</sup> It is estimated that the regulations to be issued on the use of sodium metabisulfite and similar chemicals in the near future will inevitably affect the shrimp industry adversely. Instead of synthetic additives, using natural additives that do not pose a risk to human health in foods is healthier and safer.<sup>8</sup>

Natural extracts and phenolic compounds, which are known to have no harmful effect, have recently attracted much attention as an alternative to chemicals used to delay the formation of melanosis in shrimp and increase the shelf life of the product.<sup>5,8,9</sup> Among these, chitosan appears high on the list. Chitosan is chemically similar to cellulose and is the most commonly found biopolymer after cellulose in nature. It is obtained by partial deacetylation of chitin, a natural polysaccharide found in the exoskeletons of shellfish such as crab, lobster, crayfish, and shrimp, and in the cell walls of fungi.<sup>10-15</sup>

The physicochemical properties of chitosan depend on the deacetylation degree and molecular weight.<sup>12,16</sup> Chitosan has varying viscosity, deacetylation degree (40-98%), and molecular weight (50,000-2,000,000 Da). The deacetylation degree indicates the number of deacetylated N-acetyl-D-glucosamine units relative to the total number of units.<sup>17</sup> The deacetylation degree of chitosan varies depending on the chitin source, isolation method, treatment time with sodium hydroxide, concentration, and temperatures applied in the extraction steps.<sup>18</sup>

Chitosan can significantly improve the shelf life of various foods due to its properties, such as moisture retention, film formation, and enzyme immobilization, as well as antimicrobial and antioxidant effects. In addition, studies on its use in foods have been increasing in recent years since it is biodegradable, non-toxic, and recognized as safe in foods (GRAS) by the U.S. Food and Drug Administration (FDA). Therefore, the present study aimed to employ chitosan, a well-documented natural additive, as an alternative to the currently used chemical, sodium metabisulfite, to eliminate such a critical quality problem and to examine the changes using digital image processing techniques, which are used in the detection of food spoilage in recent years, along with subjective sensory evaluations.

## MATERIALS AND METHODS

### MATERIALS

All chemicals and compounds used in the study, such as sodium metabisulfite (puriss., meets analytical specification of Ph. Eur., BP, NF, FCC, E223, dry, 97-100.5%, CAS-7681-57-4), citric acid (ACS reagent, ≥99.5%, CAS-77-92-9), acetic acid (≥99%, glacial, ReagentPlus®), HCl (37%, EMPROVE® ESSENTIAL), NaOH (≥98%, anhydrous pellets), and H<sub>2</sub>O<sub>2</sub> (30%, stabilised, EMPROVE® ESSENTIAL) were analytical grade and purchased from Merck and Sigma-Aldrich.

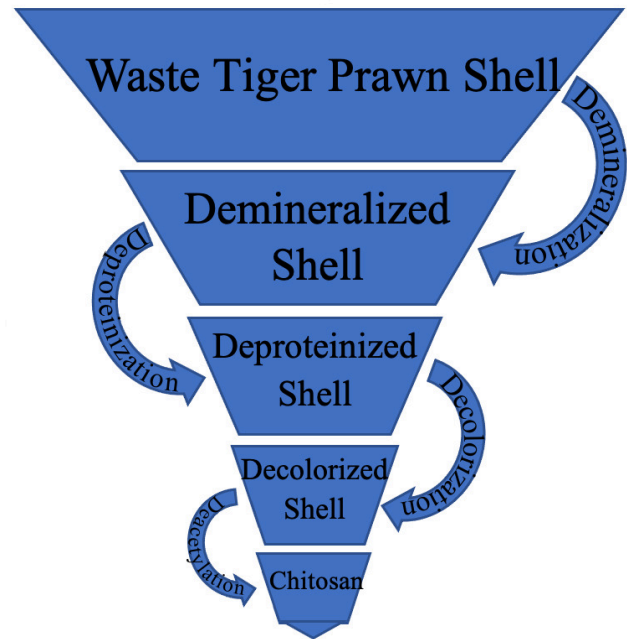


**Figure 1. Chitosan Extraction from Prawn Shell Waste by Chemical Method**

### CHITOSAN EXTRACTION AND CHARACTERIZATION

Tiger Prawn (*Penaeus semisulcatus*) shell wastes acquired from shellfish processing factories were used for chitosan extraction. Chitin was obtained from waste shells by demineralization, deproteinization, and decolorization processes with modifications in the method of Fernandez-Kim.<sup>11</sup> Chitosan was then extracted by deacetylation of chitin in an alkaline environment under high temperature and pressure. In these processes, chitosan having two different deacetylation degrees was obtained by applying 1.7N HCl for 5h, 2M NaOH for 3h, HCl:H<sub>2</sub>O<sub>2</sub> for 30 min, and 50% NaOH at 120°C at 1.25 atm pressure for 30 min and 6 h, respectively (Figure 1).

Elemental analysis, Fourier transform infrared spectroscopy (FT-IR), X-Ray diffraction analysis (XRD), scanning electron microscopy (SEM), color measurement, and dynamic viscosity analysis were performed for the characterization of the extracted chitosan. For these analyses, the methods of Kucukgulmez et al.,<sup>19</sup> Küçükgülmez et al.,<sup>20</sup> Kadak,<sup>12</sup> and Kadak et al.<sup>21</sup> were followed.

For elemental analysis, the percentages of carbon (C), hydrogen (H), and nitrogen (N) elements were determined with the Eurovector brand EA-3000 Single model instrument, and the deacetylation degree was determined using the C/N ratio. The deacetylation degree was calculated using the following formula<sup>22,23</sup>;

$$DA\% = [(C/N - 5.14)/1.72] \times 100 \quad (1)$$

$$DD\% = 100 - DA\% \quad (2)$$

Infrared characterization of chitosan was performed with Bruker brand Alpha Platinum ATR model device. The deacetylation degree was calculated with to the formula below using the values obtained at wavenumbers of 1320 cm<sup>-1</sup> and 1420 cm<sup>-1</sup> in the FT-IR analysis<sup>24</sup>;



**Figure 2. Fresh Deep-Water Rose Shrimp (*Parapenaeus longirostris*)**

$$DD\% = 100 - \left[ \frac{(A_{1320}/A_{1420}) - 0.3822}{0.03133} \right] \quad (3)$$

For viscosity measurements, chitosan solutions were prepared at 1% concentrations in 1% acetic acid, and measurements were made using Ubbelohde capillary viscometer at  $23 \pm 1$  °C.

In the color measurements of chitosan,  $L^*$ ,  $a^*$ , and  $b^*$  values were recorded according to the HunterLab Scan measurement method specified by Calder.<sup>25</sup> In this measurement system, the ' $L^*$ ' value represents brightness (whiteness-blackness or lightness-darkness), the ' $a^*$ ' value represents red color, the ' $-a^*$ ' value represents green color, the ' $+b^*$ ' value represents yellow color, and the ' $-b^*$ ' value represents blue color. At least five different points on the sample were used for each measurement. Chroma, hue, and whiteness values were calculated using average color data. Before the analysis, the instrument was calibrated with a white and a black plate.

XRD analysis was conducted by scanning between 5-50  $\theta$  values using a Bruker brand instrument.

The FEI brand Quanta FEG 250 model scanning electron microscope was used for SEM imaging. The samples' surface, which should have a conductive surface due to the analysis' working principle, was made conductive by coating with gold-palladium (Au/Pd) for 45 seconds using the Cressington Sputter Quater 108 Auto device. Imaging was performed under high vacuum, at different kV values and magnification ranges. Images obtained at 40,000x magnification were used for the examinations.

#### PREPARATION OF DEEP-WATER ROSE SHRIMP

The deep-water rose shrimp (*Parapenaeus longirostris* Lucas, 1846) specimens used in the study were obtained from the local fish market. The samples were transported to the laboratory in a Styrofoam box filled with ice (shrimp:ice, w:w, 1:2), and the day they were brought was assigned as day 0. The shrimps were recently caught, received no chemical treatment, and displayed no melanosis (Figure 2). The mean length and weight of the shrimps were measured as  $16.56 \pm 1.14$  cm and  $32.84 \pm 3.10$  g, respectively. Randomly choose three shrimp were used for each group.

#### PREPARATION OF SOLUTIONS AND TREATMENT WITH SHRIMPS

Seven different groups, consisting of 3 control groups and four different solutions, were created for the present study. The shrimps were arbitrarily taken from the Styrofoam boxes, and groups with equal samples were formed. The following group names and abbreviations were assigned: G1 (control- water), G2 (control- 1% acetic acid), G3 (control- ice), G4 (0.5% high deacetylation degree -HDD- chitosan), G5 (0.5% low deacetylation degree -LDD- chitosan), G6 (1% sodium metabisulfite), and G7 (1% citric acid).

The prepared solutions were added to the whole shrimps at a ratio of 1:1.5 (v/w) by immersion method and stored at 4 °C. Afterwards, the shrimps were drained on 40x40 cm-sized absorbent lab sheets and placed on Styrofoam plates. The plates containing shrimps were held in refrigerator conditions (+4 °C) throughout the study.

#### METHODS

##### ANALYSES OF STORED SHRIMPS

The analyses were conducted under two categories: sensory evaluation and digital image processing.

##### SENSORY EVALUATION

The melanosis index was determined with a visual assessment based on the melanosis index scale (from 0 to 10) of Otwell and Marshall.<sup>26</sup> This evaluation was carried out by seven expert panelists based on the rate of blackening on the shrimp shell surface. For this evaluation, three shrimp samples were used. The assessment scale is as follows: 0= absent, 2= slight - noticeable on some shrimps, 4= slight - noticeable on most shrimps, 6= moderate - noticeable on most shrimps, 8= heavy - noticeable on most shrimps, and 10= heavy - totally unacceptable.

##### DIGITAL IMAGE PROCESSING

Appearance assessment for color changes was carried out by examination of photographs taken throughout the storage. Obtained images were evaluated with digital image processing techniques. For this evaluation, image correction, image enhancement, classification, and data integration techniques, which enable digital images to be interpreted using various mathematical algorithms with computer assistance, are called digital image processing methods.<sup>27-29</sup>

##### IMAGE SEGMENTATION AND ALGORITHMS

Image segmentation is an image enrichment process that enables the identification of homogeneous objects on visual data by automatically separating them into sublayers.<sup>30</sup> This method was first developed by Kettig and Landgrebe.<sup>31,32</sup>

The image segmentation algorithm of the Definiens Developer software classifies pixels with similar properties into homogeneous pieces based on spectral and spatial cri-

teria. In this process, mentioning an accurate segmentation option is not possible. A large number of trials should be conducted until the segments most suitable for the purpose of the study are created. The important thing here is to establish a proper structure from the pixel to the object by providing the appropriate homogeneity. For this reason, scale, color, shape, softness, and integrity variables are used in the segmentation stage. With the help of a function including these variables, a chain structure is established from pixel to segment and from segment to larger segments.<sup>33</sup> The classification stage is initiated after the compatible fields are determined in the Definiens Developer software. At this point, an appropriate, realistic segmentation based on the sample's color differences is critical.<sup>34</sup> Therefore, it is necessary to create a structure that can express the visually closest fields with segments separated as much as possible from each other and keep the heterogeneity in balance. The segmentation process aims to work on groups of pixels with similar properties instead of just pixels and uses tissue features to distinguish the color changes/distortion in shrimp (*P. longirostris*). For this purpose, image objects are segmented using the segmentation algorithm integrated into the Definiens software. The bottom-up field-joining method was employed in the segmentation of the photographs of the *P. longirostris* taken during 12 days of storage after treatment with different preservatives.

#### SEGMENTATION ALGORITHMS

Segmentation algorithms are used to subdivide a complete image consisting of pixel-level fields or special image objects within smaller image files. Definiens offers several different approaches to solving problem sources with the help of straightforward algorithms, using various methods such as contrast segmentation or multidimensional resolution segmentation (e.g., quadtree, a non-uniform mesh generation technique, and chessboard). Segmentation algorithms are needed when it is desired to create a new image file based on the image's layer information. These algorithms become handy tools for retouching an existing image file by dividing it into smaller pieces for more detailed analysis. The 'spectral variation hypothesis' proposed by M. Palmer et al.<sup>35</sup> and M. W. Palmer et al.<sup>36</sup> states that higher spectral heterogeneity in an image corresponds to higher diversity. Tissue parameters calculated for the detection of GLCM-based melanosis confirm this hypothesis. The inputs were the segmentation scale, color, shape, integrity, and transitivity parameters. In this method, color and shape parameters and integrity and transitivity parameters take the complementary values of 1.<sup>37</sup> Several value combinations were assigned to the segmentation parameters to find the appropriate parameter values, and visual analysis was used for the decision. In the visual examination, the spatial and morphological suitability of the image objects obtained for the field were evaluated, and the segmentations that best distinguished the damaged and undamaged regions were preferred.

#### HARALICK TEXTURE

The grey-level co-occurrence matrix (GLCM) lists how often combinations of grey pixel levels differ within an image. There is a different reoccurrence matrix for each neighboring relationship. To obtain the vector constant, all four different directions (0°, 45°, 90°, 135°) are summed up before the texture calculation. The 0° angle represents the vertical direction, and the 90° angle represents the horizontal direction. In the Definiens package program, the Haralick texture is calculated for all pixels of an image file. To reduce the edge effect, the image file is subjected to an additional calculation process to include the pixels surrounded by a certain distance. Each GLCM is normalized according to the formula below. For the texture calculation of Haralick texture, the parameters were applied as follows: scale=30, shape=0.3, and compact=0.5 in the analysis within the Definiens package program. GLCM entropy texture parameters were calculated for each segment.

The Haralick image structure differs from the original pixel size of the image data. The generated dynamic array is converted to 8-bit data before the joining occurs. Although the direct use of 8-bit data will yield more reliable results, it is necessary to use dynamic data higher than 8 bits to calculate the samples' mean and standard error values. The pixel is divided into 255 equal parts within itself when 8-bit data is used for Haralick texture.

GLCM is a feature extraction method proposed by M. Haralick to extract features from a greyscale image. GLCM defines the relationship between two adjacent pixels. The first of these pixels is known as the reference pixel, and the second is the neighbor pixel.<sup>38</sup> GLCM creates a frequency matrix between two consecutive pixels in an image. The distribution in the matrix is adjusted according to the distance and angle between the pixels. This matrix is an  $N_g$ -sized square matrix, and each matrix element specifies the number of occurrences of pairs of  $i$  and  $j$  pixel values at  $d$  distance.<sup>39</sup> From these matrices, four properties, i.e., contrast, homogeneity, entropy, and brightness, were calculated to characterize the image's texture.

Texture properties calculated from GLCM;

##### i) Contrast

Contrast is heterogeneity, which is the opposite of homogeneity. Contrast is assessed by determining the amount of local variation in the image. The number of rows ( $i$ ) and columns ( $j$ ) increases in parallel with the increase in contrast.<sup>40</sup> The parameters for the calculation are as follows:

$$\sum_{i,j=0}^{N-1} P_{i,j}(i-j)^2 \quad (4)$$

In Equation 4:  $i$ = number of rows,  $j$ = number of columns,  $P_{i,j}$ = normalised  $i$  and  $j$  values,  $N$ = number of rows or columns. Value range= [0; 90].

##### ii) Homogeneity

If certain areas of a cell show homogeneity and GLCM values are concentrated in the corners, that cell has a high color value. The color values of homogeneous areas and heterogeneous areas are opposite to each other. Values decrease from heterogeneous to homogeneous areas.<sup>40</sup> The parameters for the calculation are as follows:

$$\sum_{i,j=0}^{N-1} \frac{P_{i,j}}{1+(i-j)^2} \quad (5)$$

In Equation 5:  $i$ = number of rows,  $j$ = number of columns,  $P_{i,j}$ = normalised  $i$  and  $j$  values,  $N$ = number of rows or columns. Value range= [0; 90].

### iii) Entropy

The uniform distribution of GLCM values leads to an increase in entropy value.<sup>40</sup> The parameters for the calculation are as follows:

$$\sum_{i,j=0}^{N-1} P_{i,j}(-\ln P_{i,j}) \quad (6)$$

In Equation 6:  $i$ = number of rows,  $j$ = number of columns,  $P_{i,j}$ = normalised  $i$  and  $j$  values,  $N$ = number of rows or columns. Value range= [0; 90].

### iv) Brightness

It is the sum of reflectance values, calculated for an image object and averaged by dividing by the number of pixels the image object occupies in all band layers. This feature is calculated only with positive layer values because errors will occur in the brightness value when calculated with combined data (negative and positive) in the image bands. More than one band is required for the calculation. Otherwise, the brightness value cannot be calculated.

$$w_k^B = \begin{cases} 0 \\ 1 \end{cases} \quad (7)$$

$$w^B = \sum_{k=1}^K w_k^B \quad (8)$$

$$\bar{c}(v) = \frac{1}{w^B} \sum_{k=1}^K w_k^B \bar{c}_k(v) \quad (9)$$

In Equations 7, 8, and 9:  $w_k^B$ = brightness degree of  $k$  layer,  $\bar{c}_k(v)$ = average intensity of  $v$  image object in  $k$  layer,  $ck^{min}$ = darkest intensity value of  $k$  layer,  $ck^{max}$ = brightest intensity value of  $k$  layer. Value range= [ $ck^{min}$ ;  $ck^{max}$ ].

This study analysed images of *P. longirostris* in jpeg file format. The GLCM matrices were obtained with the e-Cognition<sup>34</sup> software. The values, which included the brightness parameter among the matrices' feature vectors, constituted the calculated data of the study.

## RESULTS

### PHYSICOCHEMICAL CHARACTERIZATION OF CHITOSAN

Characterization data of chitosan extracted from shrimp shells are given in [Table 1](#).

According to the results of physicochemical analysis, the deacetylation degrees for HDD and LDD measured by two different methods were calculated as 99.5% and 76.31% in elemental analysis and 89.51% and 78.24% in FT-IR spectroscopy, respectively. Deacetylation degrees showed parallelism in both methods. The viscosity values were also measured as 0.34cSt and 4.17cSt, respectively. Chitosan's viscosity values can be significantly affected by the degree of deacetylation, solution concentration, and pH and temperature in the chitosan production.<sup>41</sup> According to the color measurements, the color values in HDD and LDD chitosan groups were 83.68 and 78.94 for  $L^*$ , 0.55 and 2.71 for  $a^*$ , 10.33 and 13.85 for  $b^*$ , respectively. The chroma val-

ues calculated with the obtained color measurements were 10.34 and 14.11, the hue values were 1.51 and 1.37, and the whiteness values were 80.67 and 74.64, respectively. While chroma indicates the intensity of color, hue angle indicates red versus yellow. Based on these data, HDD chitosan was observed to appear lighter cream-white in color than LDD chitosan.

Within the scope of the study, SEM images and FT-IR and XRD spectra were also examined for the characterization of chitosan samples extracted at different deacetylation degrees. The FT-IR and XRD analysis results are presented in [Figure 3](#), and the results of SEM images are given in [Figure 4](#).

SEM image analysis of HDD and LDD chitosan extracted within the scope of the study was performed on images obtained at 10.00kV energy level with 40.000x magnification ([Figure 4](#)).

### CHANGES DURING SHRIMP STORAGE

#### SENSORY CHANGES

The fresh shrimp samples obtained from the local fish market were transported to the laboratory in the cold chain, and all processes were carried out as rapidly as possible. Extreme precautions were taken to prevent the formation of melanosis due to external factors such as temperature and light. Equally and arbitrarily grouped shrimp specimens were stored in styrofoam boxes containing flake ice. After the treatments, the melanosis formation images obtained from the control groups (G1= water, G2= acetic acid, G3= ice), trial groups (G4= HDD chitosan, G5= LDD chitosan), and commercial preservative groups (G6= sodium metabisulfite, G7= citric acid), during the storage are presented below in [Figure 5](#).

As shown in [Figure 5](#), all shrimp samples' color and texture integrity were considerably well on the 4<sup>th</sup> day of storage. Melanosis formation is in the early stages, especially on the 6<sup>th</sup> day. Melanosis began to emerge in groups 1, 2, and 3, i.e., control groups. On the 8<sup>th</sup> day, the formation of melanosis in the first three groups was distributed throughout the body, and the development of melanosis in these groups exceeded the acceptable level. Tissue integrity started to deteriorate, especially in G1 and G2 samples. In other groups, melanosis began partially. On the 12<sup>th</sup> day, melanosis advanced in all groups, and all samples became inconsumable.

#### COLOR CHANGES

The changes in the color values of the shrimp groups immersed in different solutions and stored in refrigerator conditions are given in [Table 2](#) and [Table 3](#).

The brightness ( $L^*$ ) value, the most influential sensory value on consumer preference, was observed as the highest (51.43) in the HDD chitosan group on the first day of the study. On the contrary, the lowest brightness (48.82) on the first day was in the group treated with citric acid. It is thought that this difference is due to the acid treatment in the study, which was initiated with shrimp samples dis-

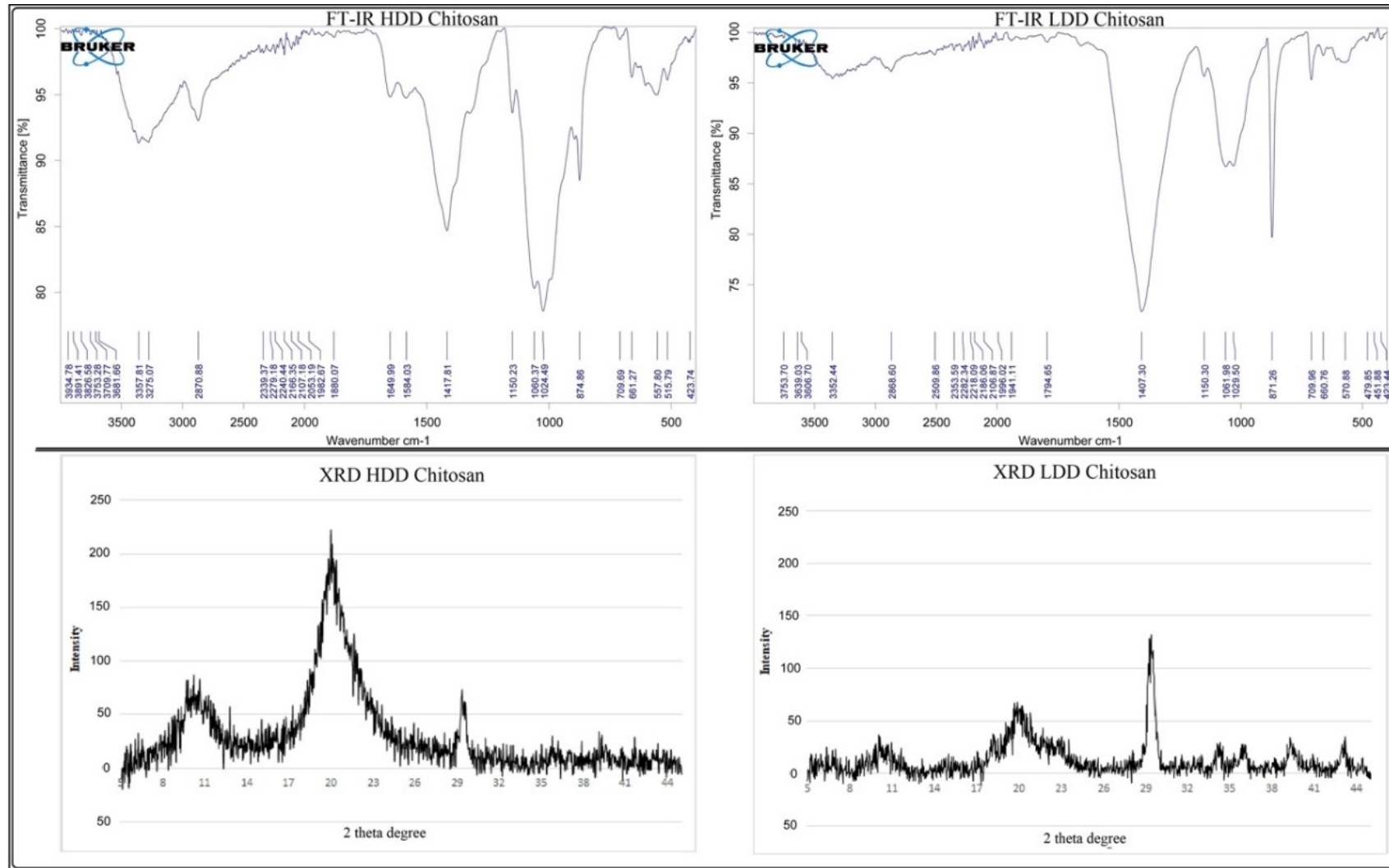


**Figure 3. FT-IR and XRD Spectrum of Chitosan with Different Deacetylation Degrees**

(HDD: High Deacetylation Degree, LDD: Low Deacetylation Degree)

**Table 1. Physicochemical Characterization Parameters of Chitosan**

		HDD Chitosan	LDD Chitosan
Deacetylation Degree (%)	Elemental	99.50	76.31
	FT-IR	89.51	78.24
Viscosity (cSt)		0.34	4.17
	L*	83.68±0.22	78.94±0.33
Color Measurement	a*	0.55±0.05	2.71±0.13
	b*	10.33±0.35	13.85±0.19
	Chroma	10.34	14.11
	Hue	1.51	1.37
	Whiteness	80.67	74.64

HDD: High Deacetylation Degree; LDD: Low Deacetylation Degree

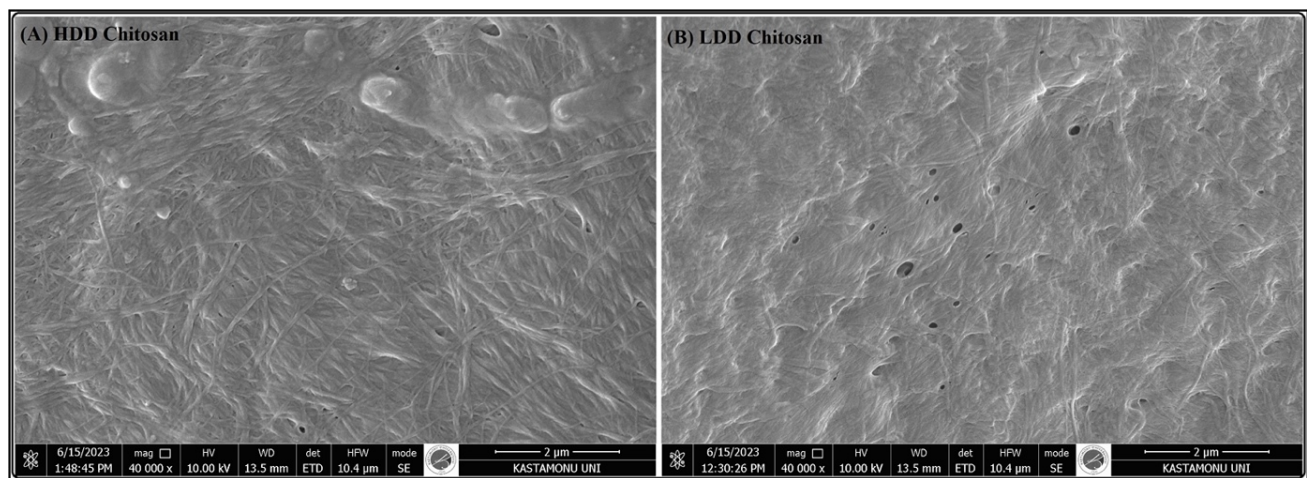


**Figure 4. SEM Images of Chitosan with Different Deacetylation Degrees (HDD: High Deacetylation Degree, LDD: Low Deacetylation Degree 40.000X)**

playing the same characteristics. The two groups with the highest brightness values on the last day of the storage were HDD (45.61) and LDD (45.83) chitosan-treated samples. The differences between the control, chitosan, sodium metabisulfite, and citric acid groups in the L\* value were statistically significant. Likewise, dullness/darkening in all groups from the first to the last day of the storage was statistically significant. The a\* value, of which negative (-) values on the color scale represent greenness and positive (+) values represent redness, increased in the positive direction in all samples. The lowest value on day 0 was 1.94 in the citric acid group, whereas the highest was 4.16 in the control-ice group. On the 12<sup>th</sup> day of the study, the highest value of 7.29 was observed in the control-water group, and the lowest value of 4.71 was observed in the HDD chitosan group. The differences between groups and within the same group on different days were statistically significant. The initial pink color on the first day gradually changed to red, and the areas where the melanosis was first observed were determined as the darkest red areas.

For this reason, the +a\* value can be proposed as another parameter of blackening occurring in deep-water rose shrimp samples. The b\* value, of which negative (-) values represent blue color and positive (+) values represent yel-

low color in the HunterLab color system, was measured in the control-water group as the lowest (10.14) on the first day of the study, while the highest was detected in the control-ice group with 12.83 on the same day. The differences between groups on the first day were statistically significant. Furthermore, the differences within all groups on different days were also significant. The lowest b\* value was detected in the HDD chitosan group at 17.73, whereas the highest was in the citric acid group at 21.77.

Chroma, hue, and whiteness values were computed using the color data obtained throughout the study. According to the calculations, the chroma value was the highest in the control-ice group, with 13.51 on day 0, and the lowest in the control-water group, with a value of 10.47. On the last day of the study, the lowest value was observed in the HDD chitosan group at 18.35, and the highest value was determined in the citric acid group at 22.96. According to the data obtained, the differences between groups on the first day of the study were statistically insignificant. However, the differences within all groups depending on the duration were determined to be statistically significant.

Regarding the hue value, at the beginning of the study, the lowest value was found in the sodium metabisulfite group at 1.24, and the highest value was determined in the

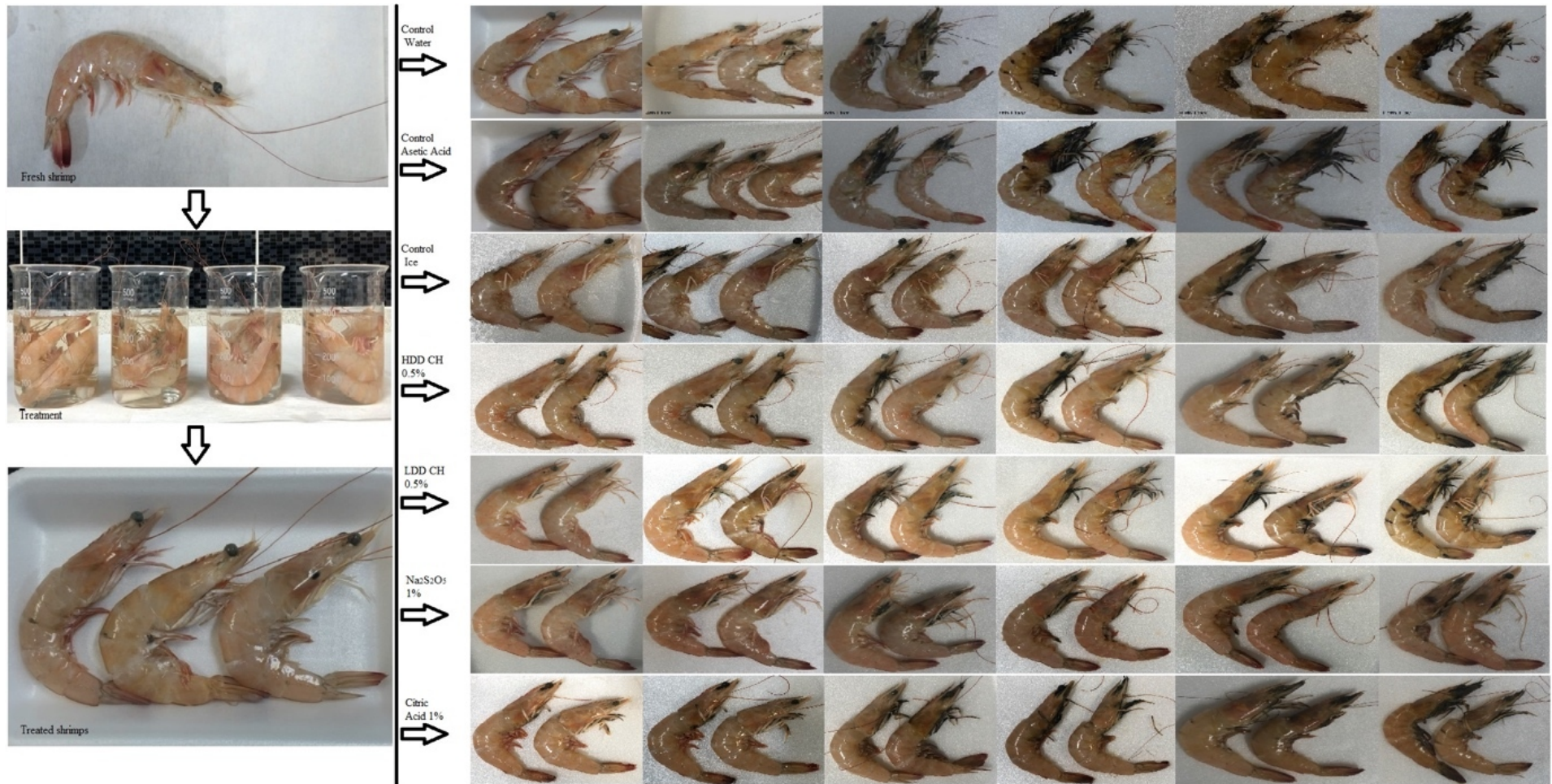


Figure 5. Processing and Melanosis Ratio of Shrimp



**Table 2. Color Changes of Deep-Water Rose Shrimp during Refrigerated Storage**

Group		Days						
		0	2	4	6	8	10	12
G1 Control Water	L*	50.25±2.13 <sup>a/x</sup>	47.37±1.08 <sup>b/x</sup>	46.76±2.14 <sup>b/x</sup>	45.81±0.36 <sup>b/x</sup>	42.25±0.074 <sup>c/x</sup>	40.75±1.74 <sup>c/x</sup>	40.98±1.89 <sup>c/x</sup>
	a*	2.47±0.80 <sup>a/xy</sup>	4.34±0.67 <sup>a/x</sup>	4.68±0.89 <sup>a/x</sup>	4.62±0.37 <sup>a/x</sup>	5.92±2.33 <sup>a/x</sup>	6.70±1.67 <sup>a/y</sup>	7.29±0.65 <sup>a/x</sup>
	b*	10.14±1.11 <sup>a/x</sup>	16.41±1.27 <sup>b/xy</sup>	17.15±1.96 <sup>b/x</sup>	19.42±4.05 <sup>b/x</sup>	20.69±3.45 <sup>b/x</sup>	20.70±2.71 <sup>b/y</sup>	21.39±3.09 <sup>b/x</sup>
G2 Control Acetic Acid	L*	50.32±2.63 <sup>a/x</sup>	48.58±0.71 <sup>ab/xy</sup>	49.06±1.64 <sup>ab/xyz</sup>	48.88±1.71 <sup>ab/x</sup>	46.30±3.14 <sup>abc/yz</sup>	45.02±3.85 <sup>bc/yzt</sup>	42.20±3.29 <sup>c/xy</sup>
	a*	3.13±1.50 <sup>ab/xy</sup>	3.79±1.27 <sup>a/x</sup>	4.31±2.06 <sup>a/x</sup>	4.15±1.94 <sup>ab/x</sup>	5.53±1.83 <sup>ab/x</sup>	6.02±0.38 <sup>ab/xy</sup>	6.72±1.02 <sup>ab/x</sup>
	b*	11.49±1.70 <sup>b/xy</sup>	14.65±1.29 <sup>ab/x</sup>	13.58±3.09 <sup>ab/x</sup>	16.32±1.13 <sup>ab/x</sup>	18.14±1.81 <sup>b/x</sup>	18.30±2.41 <sup>ab/xy</sup>	20.49±0.96 <sup>b/x</sup>
G3 Control Ice	L*	51.19±2.49 <sup>b/x</sup>	52.20±2.07 <sup>a/z</sup>	52.11±0.98 <sup>a/z</sup>	49.56±1.95 <sup>bc/x</sup>	49.21±2.29 <sup>bc/z</sup>	47.09±1.11 <sup>b/zt</sup>	43.48±1.14 <sup>c/xy</sup>
	a*	4.16±1.19 <sup>ab/y</sup>	4.24±1.78 <sup>ab/x</sup>	4.06±1.51 <sup>a/x</sup>	4.88±0.76 <sup>b/x</sup>	4.96±1.37 <sup>b/x</sup>	5.28±1.12 <sup>ab/xy</sup>	6.05±1.20 <sup>ab/x</sup>
	b*	12.83±0.63 <sup>b/y</sup>	14.13±1.65 <sup>ab/x</sup>	13.30±4.37 <sup>ab/x</sup>	16.99±4.56 <sup>b/x</sup>	17.79±3.06 <sup>ab/x</sup>	17.49±0.81 <sup>b/xy</sup>	19.09±3.63 <sup>b/x</sup>
G4 HDD CH 0.5%	L*	51.43±1.23 <sup>a/x</sup>	50.52±1.67 <sup>ab/yz</sup>	49.59±1.04 <sup>abc/xyz</sup>	48.05±3.17 <sup>bcd/x</sup>	48.14±1.12 <sup>bcd/yz</sup>	47.06±0.75 <sup>cd/zt</sup>	45.61±1.67 <sup>d/y</sup>
	a*	3.00±0.24 <sup>ab/y</sup>	4.11±1.00 <sup>ab/x</sup>	4.34±0.51 <sup>a/x</sup>	4.40±1.16 <sup>b/x</sup>	4.22±0.50 <sup>b/x</sup>	4.47±0.51 <sup>ab/x</sup>	4.71±0.28 <sup>b/x</sup>
	b*	11.85±0.46 <sup>b/xy</sup>	14.98±2.58 <sup>bcd/xy</sup>	15.29±0.96 <sup>ab/x</sup>	15.50±0.91 <sup>b/x</sup>	16.83±1.63 <sup>b/x</sup>	16.99±0.67 <sup>bc/x</sup>	17.73±3.41 <sup>bc/x</sup>
G5 LDD CH 0.5%	L*	50.66±2.21 <sup>a/x</sup>	49.81±2.06 <sup>ab/xyz</sup>	49.30±2.38 <sup>ab/xyz</sup>	49.19±2.74 <sup>ab/x</sup>	48.17±2.15 <sup>ab/yz</sup>	48.29±0.33 <sup>ab/t</sup>	45.83±1.81 <sup>b/y</sup>
	a*	3.28±0.85 <sup>bc/xy</sup>	4.48±0.66 <sup>ab/x</sup>	5.03±0.86 <sup>a/x</sup>	5.57±1.20 <sup>ab/x</sup>	5.82±0.39 <sup>b/x</sup>	6.06±0.49 <sup>ab/xy</sup>	6.04±1.20 <sup>b/x</sup>
	b*	12.52±1.20 <sup>b/xy</sup>	16.06±1.25 <sup>cde/xy</sup>	14.97±2.02 <sup>ab/x</sup>	16.12±2.68 <sup>b/x</sup>	18.11±2.50 <sup>b/x</sup>	17.35±0.82 <sup>cd/x</sup>	18.26±0.31 <sup>bc/x</sup>
G6 Na <sub>2</sub> S <sub>2</sub> O <sub>5</sub> 1%	L*	49.35±2.57 <sup>ab/x</sup>	50.78±2.06 <sup>a/yz</sup>	50.20±2.09 <sup>a/yz</sup>	49.67±2.53 <sup>a/x</sup>	45.63±2.36 <sup>bc/xyz</sup>	43.26±2.27 <sup>c/xy</sup>	42.40±0.83 <sup>c/xy</sup>
	a*	3.99±1.02 <sup>bc/y</sup>	5.82±1.21 <sup>ab/x</sup>	6.07±1.59 <sup>a/x</sup>	6.03±1.33 <sup>b/x</sup>	6.13±1.74 <sup>b/x</sup>	6.74±1.00 <sup>b/y</sup>	6.64±0.82 <sup>b/x</sup>
	b*	11.74±1.99 <sup>b/xy</sup>	14.69±0.68 <sup>dde/x</sup>	14.10±1.49 <sup>ab/x</sup>	15.05±0.18 <sup>b/x</sup>	16.85±1.31 <sup>b/x</sup>	18.14±0.93 <sup>de/xy</sup>	19.44±1.80 <sup>bc/x</sup>
G7 Citric Acid 1%	L*	48.82±2.09 <sup>a/x</sup>	48.66±1.20 <sup>a/xy</sup>	47.94±1.39 <sup>ab/xy</sup>	44.89±3.36 <sup>bc/x</sup>	44.34±1.27 <sup>c/xy</sup>	43.52±0.54 <sup>c/xyz</sup>	41.79±2.05 <sup>c/x</sup>
	a*	1.94±0.46 <sup>bc/x</sup>	4.44±0.62 <sup>b/x</sup>	4.50±1.76 <sup>a/x</sup>	5.27±2.22 <sup>b/x</sup>	5.68±1.07 <sup>b/x</sup>	5.85±0.36 <sup>b/xy</sup>	7.08±2.80 <sup>b/x</sup>
	b*	10.93±1.48 <sup>b/xy</sup>	17.73±0.59 <sup>e/y</sup>	17.04±2.72 <sup>b/x</sup>	18.90±3.23 <sup>b/x</sup>	19.69±1.12 <sup>b/x</sup>	19.28±1.97 <sup>e/xy</sup>	21.77±2.29 <sup>c/x</sup>

According to Duncan's analysis, a,b,c,d, and e indicate significant differences among samples treated with the same solution on different days, and x,y,z, and t show significant differences among groups on the same day of storage.

**Table 3. Color Changes of Deep-Water Rose Shrimp during Refrigerated Storage**

Group		Days						
		0	2	4	6	8	10	12
G1 Control Water	Chroma	10.47±0.94 <sup>a/x</sup>	16.99±1.08 <sup>b/xy</sup>	17.78±2.12 <sup>bc/x</sup>	19.97±4.02 <sup>bc/x</sup>	21.62±3.34 <sup>bc/x</sup>	21.82±2.44 <sup>bc/y</sup>	22.61±3.08 <sup>c/x</sup>
	Hue	1.32±0.09 <sup>a/xy</sup>	1.31±0.05 <sup>a/x</sup>	1.30±0.02 <sup>a/y</sup>	1.33±0.03 <sup>a/y</sup>	1.29±0.11 <sup>a/x</sup>	1.25±0.09 <sup>a/xy</sup>	1.24±0.03 <sup>a/x</sup>
	Whiteness	49.16±2.28 <sup>a/x</sup>	44.68±0.83 <sup>b/x</sup>	43.83±1.45 <sup>b/x</sup>	42.16±0.97 <sup>b/xy</sup>	38.28±1.46 <sup>c/x</sup>	39.81±1.07 <sup>c/x</sup>	36.75±2.21 <sup>c/x</sup>
G2 Control Acetic Acid	Chroma	11.96±1.80 <sup>a/xy</sup>	15.17±1.22 <sup>abc/x</sup>	14.29±3.50 <sup>ab/x</sup>	16.89±1.51 <sup>bcd/x</sup>	18.99±2.23 <sup>cde/x</sup>	19.27±2.38 <sup>de/xy</sup>	21.60±1.23 <sup>e/x</sup>
	Hue	1.30±0.11 <sup>a/xy</sup>	1.32±0.08 <sup>a/x</sup>	1.27±0.09 <sup>a/xy</sup>	1.32±0.09 <sup>a/xy</sup>	1.28±0.07 <sup>a/x</sup>	1.25±0.03 <sup>a/xy</sup>	1.25±0.03 <sup>a/x</sup>
	Whiteness	48.88±2.52 <sup>b/x</sup>	46.39±1.02 <sup>ab/xy</sup>	47.01±1.24 <sup>a/yz</sup>	46.14±1.20 <sup>ab/xy</sup>	42.98±2.42 <sup>ab/yz</sup>	41.67±2.92 <sup>a/yz</sup>	38.26±2.67 <sup>ab/x</sup>
G3 Control Ice	Chroma	13.51±0.94 <sup>a/y</sup>	14.79±2.04 <sup>ab/x</sup>	13.91±4.61 <sup>ab/x</sup>	17.68±4.56 <sup>ab/x</sup>	18.47±3.31 <sup>ab/x</sup>	18.30±0.49 <sup>ab/x</sup>	20.02±3.82 <sup>b/x</sup>
	Hue	1.26±0.07 <sup>a/xy</sup>	1.28±0.09 <sup>a/x</sup>	1.27±0.02 <sup>a/xy</sup>	1.28±0.03 <sup>a/xy</sup>	1.30±0.02 <sup>a/x</sup>	1.27±0.07 <sup>a/xy</sup>	1.26±0.00 <sup>a/x</sup>
	Whiteness	49.35±2.63 <sup>b/x</sup>	49.93±2.02 <sup>ab/z</sup>	50.00±1.53 <sup>a/</sup>	46.47±3.34 <sup>abc/xy</sup>	45.92±3.31 <sup>ab/z</sup>	44.01±0.96 <sup>a/z</sup>	39.97±1.90 <sup>abc/xy</sup>
G4 HDD CH 0.5%	Chroma	12.23±0.41 <sup>a/xy</sup>	15.56±2.53 <sup>b/xy</sup>	15.90±0.84 <sup>b/x</sup>	16.15±0.78 <sup>b/x</sup>	17.27±1.68 <sup>b/x</sup>	17.57±0.70 <sup>b/x</sup>	18.35±3.26 <sup>b/x</sup>
	Hue	1.32±0.02 <sup>a/xy</sup>	1.30±0.07 <sup>a/x</sup>	1.29±0.04 <sup>a/xy</sup>	1.29±0.08 <sup>a/xy</sup>	1.34±0.01 <sup>a/x</sup>	1.31±0.02 <sup>a/y</sup>	1.30±0.04 <sup>a/x</sup>
	Whiteness	49.91±1.16 <sup>b/x</sup>	48.08±1.47 <sup>ab/yz</sup>	47.13±1.15 <sup>ab/yz</sup>	45.59±2.92 <sup>bcd/xy</sup>	45.33±1.55 <sup>ab/z</sup>	44.21±0.91 <sup>a/z</sup>	42.55±2.62 <sup>bcd/y</sup>
G5 LDD CH 0.5%	Chroma	12.96±1.30 <sup>a/xy</sup>	16.69±1.04 <sup>b/xy</sup>	15.80±2.08 <sup>ab/x</sup>	17.07±2.82 <sup>b/x</sup>	19.03±2.42 <sup>b/x</sup>	18.38±0.89 <sup>b/x</sup>	19.24±0.69 <sup>b/x</sup>
	Hue	1.31±0.05 <sup>a/xy</sup>	1.30±0.06 <sup>a/x</sup>	1.24±0.04 <sup>a/xy</sup>	1.23±0.05 <sup>a/xy</sup>	1.25±0.04 <sup>a/x</sup>	1.23±0.02 <sup>a/xy</sup>	1.25±0.05 <sup>a/x</sup>
	Whiteness	48.98±2.31 <sup>c/x</sup>	47.09±1.83 <sup>bc/xyz</sup>	46.85±1.66 <sup>ab/xyz</sup>	46.33±1.71 <sup>bcd/xy</sup>	44.73±1.34 <sup>bc/yz</sup>	45.12±0.61 <sup>b/t</sup>	42.50±1.68 <sup>cd/y</sup>
G6 Na <sub>2</sub> S <sub>2</sub> O <sub>5</sub> 1%	Chroma	12.40±2.19 <sup>a/xy</sup>	15.83±0.74 <sup>b/xy</sup>	15.38±1.91 <sup>b/x</sup>	16.24±0.63 <sup>b/x</sup>	17.96±1.84 <sup>bc/x</sup>	19.36±1.12 <sup>c/xy</sup>	20.55±1.88 <sup>c/x</sup>
	Hue	1.24±0.03 <sup>a/x</sup>	1.19±0.07 <sup>a/x</sup>	1.17±0.07 <sup>a/x</sup>	1.19±0.07 <sup>a/x</sup>	1.22±0.06 <sup>a/x</sup>	1.21±0.04 <sup>a/x</sup>	1.24±0.03 <sup>a/x</sup>
	Whiteness	47.84±2.94 <sup>c/x</sup>	48.29±2.10 <sup>cd/yz</sup>	47.87±2.23 <sup>bc/yz</sup>	47.11±2.50 <sup>cd/y</sup>	42.73±2.81 <sup>bc/yz</sup>	40.04±2.36 <sup>b/y</sup>	38.83±0.86 <sup>d/xy</sup>
G7 Citric Acid 1%	Chroma	11.12±1.36 <sup>a/xy</sup>	18.29±0.47 <sup>b/y</sup>	17.71±2.46 <sup>b/x</sup>	19.66±3.61 <sup>bc/x</sup>	20.51±1.18 <sup>bc/x</sup>	20.15±1.96 <sup>bc/xy</sup>	22.96±2.90 <sup>c/x</sup>
	Hue	1.39±0.07 <sup>a/y</sup>	1.32±0.04 <sup>a/x</sup>	1.30±0.12 <sup>a/y</sup>	1.30±0.08 <sup>a/xy</sup>	1.29±0.05 <sup>a/x</sup>	1.27±0.02 <sup>a/xy</sup>	1.26±0.09 <sup>a/x</sup>
	Whiteness	47.63±2.33 <sup>c/x</sup>	45.50±1.21 <sup>d/xy</sup>	45.00±2.11 <sup>c/xy</sup>	41.45±4.29 <sup>d/x</sup>	40.67±1.38 <sup>b/xy</sup>	40.01±0.91 <sup>b/y</sup>	37.39±2.74 <sup>d/x</sup>

According to Duncan's analysis, a,b,c,d, and e indicate significant differences among samples treated with the same solution on different days, and x,y,z, and t show significant differences among groups on the same day of storage.

citric acid group at 1.39. On the last day, these values were the lowest in the sodium metabisulfite and control-water groups, with 1.24, and the highest in the HDD chitosan group, with 1.30. There was no statistically significant difference in the hue value between the groups on the first and last days of the study. Another calculated parameter is whiteness. According to the whiteness calculations, the lowest value was found in the citric acid group, with 47.63 on the first day, and the highest value was determined in the HDD chitosan group, with 49.91 on the same day. On the last day of the study, the lowest value (36.75) was obtained in the control-water group, and the highest value (42.55) was obtained in the HDD chitosan group. The differences detected between groups and between days were found to be statistically significant both at the beginning and end of the study.

#### DIGITAL IMAGE PROCESSING

The results of the image processing analysis, conducted in addition to the subjective results obtained in the sensory evaluation, are given in [Figure 6](#).

The results obtained through the image processing analysis showed parallelism with the results obtained through the sensory evaluation. According to the analysis results, less than 1% of the total surface area was detected as a melanosis formation region in the fresh sample. This value was determined as 10.55%, 7.72%, and 9.87% in the G1, G2, and G3 control groups, respectively, on the last day of the study. The lowest levels in the study were determined to be in the G4 and G5 groups, representing groups treated with chitosan, remaining at 0.30% and 0.02, respectively. On the other hand, it was determined as 1.54% and 4.01% in the G6 and G7 groups, consisting of the most widely used commercial preservatives (i.e., sodium metabisulfite and citric acid) for the prevention of melanosis formation in shrimps, respectively. The image processing analysis results obtained in the study revealed that commercial chemicals, i.e., sodium metabisulfite and citric acid, were effective in delaying the formation of melanosis in deep-water rose shrimp; however, the most effective additives were natural HDD and LDD chitosan.

#### DISCUSSION

Chitosan, the most common biopolymer in nature after cellulose, has a wide range of applications due to its properties. It can be used in many areas, including agriculture, food, cosmetics, pharmacy, medicine, and engineering. The primary sources of chitosan and its derivatives are fungi, shellfish and some terrestrial animals (e.g., insects).<sup>42-44</sup> When choosing the preparation method of chitosan, a functionalised method suitable for the purpose should be preferred. It is mandatory to determine the product's properties to be used in a study each time because it can be obtained from many different sources, and its unique functional properties vary depending on the production method. For this reason, to begin with, the physicochemical properties of chitosan were determined. The deacetylation

degrees of the extracted chitosan used in the study, determined by two different methods, were 99.50 and 89.51% for high deacetylation degree and 76.31 and 78.24% for low deacetylation degree. In addition to the deacetylation degree, viscosity and color values were found to be similar to the values obtained both in commercial products and in other previous research.<sup>17,45-53</sup>

FT-IR spectroscopy is used for the identification of organic compounds. The IR spectrum of all compounds is different except for optical isomers, and the IR region is located between the visible light and microwave regions in the electromagnetic spectrum. This region is between 4000-450 $\text{cm}^{-1}$  wavelength. The peak values obtained in the study, i.e., between 423 $\text{cm}^{-1}$ , 661 $\text{cm}^{-1}$ , and 660 $\text{cm}^{-1}$ , are named "fingerprint peaks" of chitosan with two different deacetylation degrees, HDD and LDD, respectively. The spectrum expressing the C2 position (C=O) of glucosamines, one of the main groups of chitosan compounds, was observed at 1024 $\text{cm}^{-1}$  and 1029 $\text{cm}^{-1}$  wavelengths. The absorbance value representing the C-O-C bonds in the ring structure was determined at 1150 $\text{cm}^{-1}$  wavelength in both samples. The absorbances specified as the stretching vibration peak in the CH<sub>2</sub> group were observed at 1417 $\text{cm}^{-1}$  and 1407 $\text{cm}^{-1}$  wavelengths. C=O-C-N bonds were only detected in HDD chitosan at a wavelength of 1584  $\text{cm}^{-1}$ . Moreover, the peaks representing OH bonds in hydroxyl groups were observed between 3275 $\text{cm}^{-1}$  and 3357 $\text{cm}^{-1}$  in HDD chitosan, while they were observed only at 3352 $\text{cm}^{-1}$  in LDD chitosan ([Figure 3](#)). The FT-IR analysis results of similar studies in the existing literature are consistent with the present study.<sup>12,19,21,46,53,54</sup>

XRD analysis is based on the principle that each crystal refracts x-rays in a characteristic pattern, depending on the specific atomic arrangement of the phase. The crystallinity of chitin and chitosan consists of two main peaks due to hydrogen bonds between the hydroxyl and N-acetyl main groups.<sup>55</sup> The main characteristic chitosan peak may not appear in the analysis results in some cases due to disruption of the interpolymer bands. It was observed in the present study that chitosan obtained from different shellfish products displayed two main characteristic crystalline peaks ([Figure 3](#)).

SEM image analysis of HDD and LDD chitosan extracted within the scope of the study was performed on images obtained at 10.00kV energy level with 40.000x magnification ([Figure 4](#)). It was observed that the morphological properties of chitosan samples varied with the change in deacetylation degrees. In general, in terms of morphology, it was visible that the filamentous structure of chitosan increased in the higher deacetylation degree. These structural differences may have emerged according to the method used and deacetylation degree or may be species-specific. In a similar study, where chemical extraction of chitosan was performed on shrimp and crayfish shells, it was stated that the surface morphologies of chitosan obtained from different sources were different according to the SEM results. It was reported that the surface of the chitosan obtained from shrimp shells displayed a smoother appearance, whereas

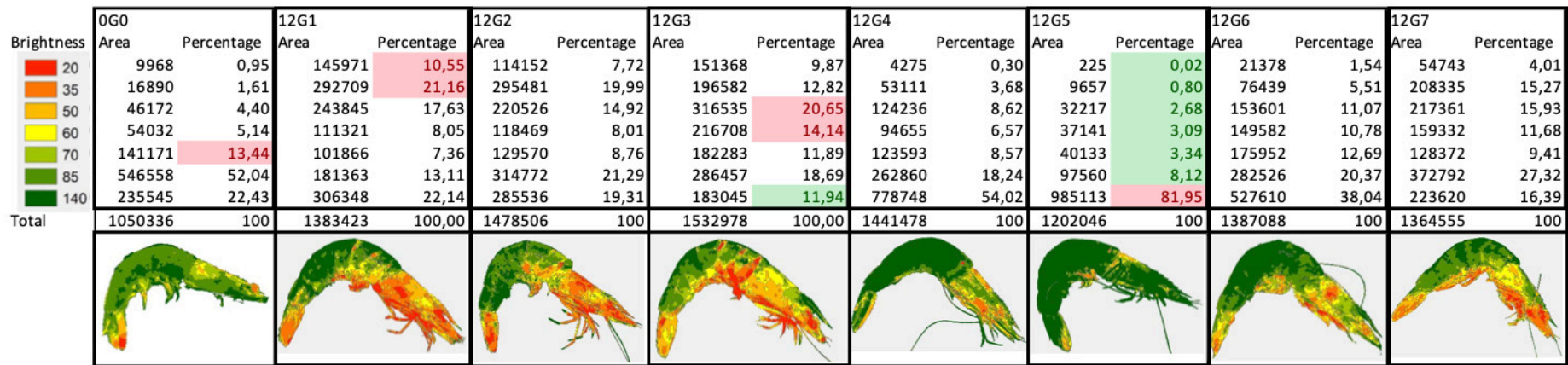


Figure 6. Image Analysis of Melanosis Rate for Fresh and 12th Day of Stored Shrimp

the chitosan obtained from crayfish shells had a three-dimensional surface appearance.<sup>47,54,56</sup>

The second phase of the research was conducted to determine whether the characterized chitosan and other widely used chemicals prevent melanosis in shrimp. Chitosan and other chemicals were applied to freshly obtained shrimp samples by immersion. Shrimps prepared this way were stored refrigerated for 12 days, and melanosis formation was monitored. The melanosis degree in shrimps was assessed according to the sensory evaluation scale of Otwell and Marshall.<sup>26</sup> According to the evaluation results in this scale, positive effects of both chitosan groups, sodium metabisulfite, and citric acid groups were observed in delaying melanosis. After the 6<sup>th</sup> day of the storage, it was determined that the groups treated with 0.5% LDD chitosan and sodium metabisulfite were in a notably better condition than the others.

On the other hand, the high deacetylation degree chitosan group exhibited a lower impact than these two groups. In general, it was observed that both high and low deacetylation degrees of chitosan are effective in delaying the formation of melanosis. Similar to the findings presented here, Bingöl et al.<sup>57</sup> found in their study on the quality of frozen shrimps treated with chitosan that samples from all groups were consumable, even at the end of the storage period, according to the panelist evaluations. However, they reported that the control group samples received lower taste and odor scores than the treatment groups. Arancibia et al.<sup>58</sup> investigated the melanosis change in shrimp (*Penaeus vannamei*) during storage with chitosan obtained from *Litopenaeus vannamei* processing wastes. They reported no variations among groups until the 5<sup>th</sup> day of storage, but the sensory properties declined drastically after the 5<sup>th</sup> day. In agreement with the present results, they reported that the chitosan-treated groups were in better condition than the control group.

Similarly, Imansari et al.<sup>59</sup> aimed to prevent melanosis formation using mangrove plant extract during cold storage of shrimps. As a result of their study, it was concluded that mangrove plant extract can delay melanosis formation. Other researchers have also reported that melanosis formation is decelerated with different natural additives.<sup>58,60-62</sup>

The results obtained in sensory evaluation were supported by digital image processing analysis. This analysis method, which was employed for the first time in this kind of study, was carried out using E-cognition (by Definiens Developer) software. E-cognition software creates pixel segments by integrating image pixels according to their different properties (color, brightness, scale, shape, softness, etc.). Created pixel segments are classified according to their properties. The classified areas are distinguished by using segmentation algorithms, and the areas of distortion/color change are thusly determined. The image processing analysis results obtained in the study revealed that commercial chemicals, i.e., sodium metabisulfite and citric

acid, were effective in delaying the formation of melanosis in deep-water rose shrimp; however, the most effective additives were natural HDD and LDD chitosan. Several studies have been carried out with chemical preservatives to decelerate the deterioration that occurs during the long shelf life, and favorable results have been obtained.<sup>60,61,63-65</sup> However, it is possible to prevent melanosis and similar undesirable changes by utilizing natural products rather than chemical preservatives. Considering the increased shrimp capture and consumption in recent years, storage needs and increasing shelf life with natural additives are very important. Furthermore, it is critical to determine the quality of the products offered to the market rapidly and objectively.

To conclude, shrimps are captured in high quantities in our country, offered to the domestic market, and exported abroad. However, shrimp is an easily perishable food with a limited shelf life. The enzymatically shaped “melanosis” or “black spot,” which begins immediately after capture, is the leading factor limiting the shelf life. The development of methods to preserve the quality of this valuable food source for a more extended period or improvement in existing methods are among the primary expectations of the respective industry. In this study, along with commercially used sodium metabisulfite and citric acid, the effect of chitosan obtained from shrimp waste on this undesired quality change was investigated, and it was concluded that it would be appropriate to use such natural substances instead of commercial preservatives. In addition to the subjective panelist evaluation, this result was also demonstrated by digital image processing techniques, which enable obtaining fast, reliable, and objective results with the help of developing technology.

#### DATA AVAILABILITY STATEMENT

The data are contained within the article, and the corresponding author can make more data available upon request.

#### CONFLICTS OF INTEREST

The author declared no conflict of interest.

#### AUTHOR CONTRIBUTION PER CREDIT

Investigation: Ali Eslem Kadak (Lead). Resources: Ali Eslem Kadak (Lead). Methodology: Ali Eslem Kadak (Lead). Formal Analysis: Ali Eslem Kadak (Lead). Visualization: Ali Eslem Kadak (Lead). Writing – original draft: Ali Eslem Kadak (Lead). Writing – review & editing: Ali Eslem Kadak (Lead). Funding acquisition: Ali Eslem Kadak (Lead).

Submitted: August 23, 2023 CDT, Accepted: September 17, 2023 CDT



This is an open-access article distributed under the terms of the Creative Commons Attribution 4.0 International License (CCBY-NC-ND-4.0). View this license's legal deed at <https://creativecommons.org/licenses/by-nc-nd/4.0> and legal code at <https://creativecommons.org/licenses/by-nc-nd/4.0/legalcode> for more information.

## REFERENCES

1. FAO. *The State of World Fisheries and Aquaculture.: Food and Agriculture Organization of the United Nations*. Food and Agriculture Organization of the United Nations; 2022.
2. TÜİK. *Su Ürünleri İstatistikleri*. Türkiye İstatistik Kurumu; 2021. <https://data.tuik.gov.tr/Bulten/Index?p=Su-Urunleri2021-45745>
3. Alparslan Y, Baygar T. Effect of chitosan film coating combined with orange peel essential oil on the shelf life of deepwater pink shrimp. *Food Bioprocess Technol*. 2017;10(5):842-853. [doi:10.1007/s11947-017-1862-y](https://doi.org/10.1007/s11947-017-1862-y)
4. Martínez-Alvarez O, Montero P, Gómez-Guillén M del C. Controlled atmosphere as coadjuvant to chilled storage for prevention of melanosis in shrimps (*Parapenaeus longirostris*). *Eur Food Res Technol*. 2004;220(2):125-130. [doi:10.1007/s00217-004-1015-1](https://doi.org/10.1007/s00217-004-1015-1)
5. Nirmal NP, Benjakul S. Melanosis and quality changes of Pacific white shrimp (*Litopenaeus vannamei*) treated with catechin during iced storage. *J Agric Food Chem*. 2009;57(9):3578-3586. [doi:10.1021/jf900051e](https://doi.org/10.1021/jf900051e)
6. Yuan G, Lv H, Tang W, Zhang X, Sun H. Effect of chitosan coating combined with pomegranate peel extract on the quality of Pacific white shrimp during iced storage. *Food Control*. 2016;59:818-823. [doi:10.1016/j.foodcont.2015.07.011](https://doi.org/10.1016/j.foodcont.2015.07.011)
7. Erkan N, Özden Ö, Alakavuk D, Tosun Ş., Varlık C, Baygar T. Determination of the total sodium metabisulphide level of shrimps sold in Istanbul. *Journal of Fisheries Sciences.com*. 2007;1(1):26-33. [doi:10.3153/jfscom.2007004](https://doi.org/10.3153/jfscom.2007004)
8. Nirmal NP, Benjakul S. Effect of catechin and ferulic acid on melanosis and quality of Pacific white shrimp subjected to prior freeze-thawing during refrigerated storage. *Food Control*. 2010;21(9):1263-1271. [doi:10.1016/j.foodcont.2010.02.015](https://doi.org/10.1016/j.foodcont.2010.02.015)
9. Gokoglu N, Yerlikaya P. Inhibition effects of grape seed extracts on melanosis formation in shrimp (*Parapenaeus longirostris*). *Int J of Food Sci Tech*. 2008;43(6):1004-1008. [doi:10.1111/j.1365-2621.2007.01553.x](https://doi.org/10.1111/j.1365-2621.2007.01553.x)
10. Altun Ş, Kadak AE, Küçükgülmez A, Gülnaz O, Çelik M. Explanantion of difenocanazole removal by chitosan with Langmuir adsorption isotherm and kinetic modeling. *Toxicol Res*. 2023;39(1):127-133. [doi:10.1007/s43188-022-00152-2](https://doi.org/10.1007/s43188-022-00152-2)
11. Fernandez-Kim SO. *Physicochemical and Functional Properties of Crawfish Chitosan as Affected by Different Processing Protocols*. Louisiana State University and Agricultural & Mechanical College; 2004.
12. Kadak AE. *Extraction and Characterization of Chitosan Biopolymer from Different Shellfish Wastes and Edible Film Production and Physicochemical Properties*. PhD Thesis. Çukurova University; 2017.
13. Küçükgülmez A, Kadak AE, Gökçin M. Antioxidative and antimicrobial activities of shrimp chitosan on gilthead sea bream (*S parus aurata*) during refrigerated storage. *Int J of Food Sci Tech*. 2013;48(1):51-57. [doi:10.1111/j.1365-2621.2012.03157.x](https://doi.org/10.1111/j.1365-2621.2012.03157.x)
14. Perera KY, Jaiswal AK, Jaiswal S. Biopolymer-Based Sustainable Food Packaging Materials: Challenges, Solutions, and Applications. *Foods*. 2023;12(12):2422. [doi:10.3390/foods12122422](https://doi.org/10.3390/foods12122422)
15. Shepherd R, Reader S, Falshaw A. Chitosan functional properties. *Glycoconjugate journal*. 1997;14(4):535-542. [doi:10.1023/a:1018524207224](https://doi.org/10.1023/a:1018524207224)
16. Duman S, Şenel S. Kitosan ve veteriner alandaki uygulamaları. *Veteriner Cerrahi Dergisi*. 2004;10(3-4):62-72.
17. Küçükgülmez A, Kadak AE, Celik L, Farivar A, Celik M. Comparison of the physicochemical properties of chitosan extracted from shrimp shell waste with different deacetylation degrees. *Feb-Fresenius Environmental Bulletin*. 2017;26(12):7750-7755.
18. Oberoi K, Tolun A, Altintas Z, Sharma S. Effect of alginate-microencapsulated hydrogels on the survival of lactobacillus rhamnosus under simulated gastrointestinal conditions. *Foods*. 2021;10(9):1999. [doi:10.3390/foods10091999](https://doi.org/10.3390/foods10091999)
19. Kucukgulmez A, Celik M, Yanar Y, Sen D, Polat H, Kadak AE. Physicochemical characterization of chitosan extracted from *Metapenaeus stebbingi* shells. *Food Chemistry*. 2011;126(3):1144-1148. [doi:10.1016/j.foodchem.2010.11.148](https://doi.org/10.1016/j.foodchem.2010.11.148)
20. Küçükgülmez A, Gülnaz O, Celik M, Yanar Y, Eslem Kadak A, Gerçek G. Antimicrobial activity of the chitosan extracted from *Metapenaeus stebbingi* shell wastes. *J Polym Environ*. 2012;20(2):431-437. [doi:10.1007/s10924-011-0395-0](https://doi.org/10.1007/s10924-011-0395-0)

21. Kadak AE, Küçükgülmez A, Ccedil;elik M. Preparation and Characterization of Crayfish (*Astacus leptodactylus*) Chitosan with Different Deacetylation Degrees. *Iranian Journal of Biotechnology*. 2023;21(2):3253. [doi:10.30498/ijb.2023.323958.3253](https://doi.org/10.30498/ijb.2023.323958.3253)
22. Abd Razak NH, Shukori NWM, Hamid KHK. Elemental Analysis of Chitin from Extraction of Different Ages of *Leucaena Leucephala* with Hydrochloric Acid. *Journal of Advanced Research in Applied Sciences and Engineering Technology*. 2019;16(1):20-25.
23. Divya K, Rebello S, Jisha M. A simple and effective method for extraction of high purity chitosan from shrimp shell waste. Paper presented at: the Proceedings of the international conference on advances in applied science and environmental engineering-ASEE; 2014.
24. Brugnerotto J, Lizardi J, Goycoolea FM, Argüelles-Monal W, Desbrières J, Rinaudo M. An infrared investigation in relation with chitin and chitosan characterization. *Polymer*. 2001;42(8):3569-3580. [doi:10.1016/s0032-3861\(00\)00713-8](https://doi.org/10.1016/s0032-3861(00)00713-8)
25. Calder BL. *The Use of Polyphosphates to Maintain Yield and Quality of Whole Cooked, Cryogenically Frozen Lobster (Homarus Americanus) and the Use of Sorbitol and Tocopherol to Maintain Quality of Whole Cooked, Cryogenically Frozen Crab (Cancer Irroratus)*. The University of Maine; 2003.
26. Otwell WS, Marshall M. Screening alternatives to sulfiting agents to control shrimp melanosis. In: *Technical Paper N°46, Studies on the Use of Sulfites to Control Shrimp Melanosis*. Florida Sea Grant College; 1986:1-10.
27. Lillesand T, Kiefer RW, Chipman J. *Remote Sensing and Image Interpretation*. John Wiley & Sons; 2015.
28. Mert A. *Ormanın yapısal çeşitliliğinin uydu verileri kullanılarak kestirimi*. Süleyman Demirel Üniversitesi Fen Bilimleri Enstitüsü; 2014.
29. Mert A, Aksan Ş, Özkan UY, Özdemir İ. Relationships between the richness of bird species and structural diversity from satellite images of Landsat-8 OLI. *Turk J For*. 2016;17(1):68-72. [doi:10.18182/tjf.03309](https://doi.org/10.18182/tjf.03309)
30. McCormick N. Satellite-based forest mapping using the SILVICS software. *User Manual Space Applications Institute, Joint Research Centre, Ispra*. 1999;307.
31. Kettig RL, Landgrebe DA. Classification of multispectral image data by extraction and classification of homogeneous objects. *IEEE Trans Geosci Electron*. 1976;14(1):19-26. [doi:10.1109/tge.1976.294460](https://doi.org/10.1109/tge.1976.294460)
32. Holmgren J. Prediction of tree height, basal area and stem volume in forest stands using airborne laser scanning. *Scandinavian Journal of Forest Research*. 2004;19(6):543-553. [doi:10.1080/02827580410019472](https://doi.org/10.1080/02827580410019472)
33. Rego LFG. Automatic Land Cover Classification Derived from High-resolution Ikonos Satellite Image in the Urban Atlantic Forest in Rio de Janeiro, Brasil by Means of an Objects-oriented Approach. Published online 2003.
34. Definiens. *Definiens Imaging Developer 7*. eCognition Software. EII Earth; 2007.
35. Palmer M, Wohlgemuth T, Earls P, Arévalo J, Thompson S. Opportunities for long-term ecological research at the Tallgrass Prairie Preserve, Oklahoma. Paper presented at: the Proceedings of the ILTER regional workshop: cooperation in long term ecological research in Central and Eastern Europe; 1999.
36. Palmer MW, Earls PG, Hoagland BW, White PS, Wohlgemuth T. Quantitative tools for perfecting species lists. *Environmetrics*. 2002;13(2):121-137. [doi:10.1002/env.516](https://doi.org/10.1002/env.516)
37. Tian J, Chen DM. Optimization in multi-scale segmentation of high-resolution satellite images for artificial feature recognition. *International Journal of Remote Sensing*. 2007;28(20):4625-4644. [doi:10.1080/01431160701241746](https://doi.org/10.1080/01431160701241746)
38. Horng MH. Texture feature coding method for texture classification. *Opt Eng*. 2003;42(1):228. [doi:10.1117/1.1527932](https://doi.org/10.1117/1.1527932)
39. Roumi M. *Implementing Texture Feature Extraction Algorithms on Fpga*. Ms. C Thesis. Department of Electrical Engineering, Faculty of Electrical Engineering, Mathematics and Computer Science, Delft University of Technology; 2009.
40. Haralick RM, Shanmugam K, Dinstein I. Textural features for image classification. *IEEE Trans Syst, Man, Cybern*. 1973;SMC-3(6):610-621. [doi:10.1109/tsmc.1973.4309314](https://doi.org/10.1109/tsmc.1973.4309314)
41. Seo S. *Depolymerization and Decolorization of Chitosan by Ozone Treatment*. Master Thesis. Chung-Ang University; 2006.

42. Ardean C, Davidescu CM, Nemeş NS, et al. Factors influencing the antibacterial activity of chitosan and chitosan modified by functionalization. *IJMS*. 2021;22(14):7449. doi:10.3390/ijms22147449
43. Azmana M, Mahmood S, Hilles AR, Rahman A, Arifin MAB, Ahmed S. A review on chitosan and chitosan-based bionanocomposites: Promising material for combatting global issues and its applications. *International Journal of Biological Macromolecules*. 2021;185:832-848. doi:10.1016/j.ijbiomac.2021.07.023
44. Kou SG, Peters LM, Mucalo MR. Chitosan: A review of sources and preparation methods. *International Journal of Biological Macromolecules*. 2021;169:85-94. doi:10.1016/j.ijbiomac.2020.12.005
45. Abdel-Rahman RM, Hrdina R, Abdel-Mohsen AM, et al. Chitin and chitosan from Brazilian Atlantic Coast: Isolation, characterization and antibacterial activity. *International Journal of Biological Macromolecules*. 2015;80:107-120. doi:10.1016/j.ijbiomac.2015.06.027
46. Ahing FA, Wid N. Extraction and characterization of chitosan from shrimp shell waste in Sabah. *Transactions on Science and Technology*. 2016;3(1-2):227-237.
47. Ghannam HE, S. Talab A, V. Dolgano N, M.S. Husse A, Abdelmagui NM. Characterization of chitosan extracted from different crustacean shell wastes. *J of Applied Sciences*. 2016;16(10):454-461. doi:10.3923/jas.2016.454.461
48. Hossain M, Iqbal A. Production and characterization of chitosan from shrimp waste. *J Bangladesh Agric Univ*. 2014;12(1):153-160. doi:10.3329/jbau.v12i1.21405
49. Hsu C, Chen S, Chen W, Tsai M, Chen R. Effect of the characters of chitosans used and regeneration conditions on the yield and physicochemical characteristics of regenerated products. *IJMS*. 2015;16(4):8621-8634. doi:10.3390/ijms16048621
50. Jeon YJ, Kamil JYVA, Shahidi F. Chitosan as an edible invisible film for quality preservation of herring and Atlantic cod. *J Agric Food Chem*. 2002;50(18):5167-5178. doi:10.1021/jf011693i
51. Marei NH, El-Samie EA, Salah T, Saad GR, Elwahy AHM. Isolation and characterization of chitosan from different local insects in Egypt. *International Journal of Biological Macromolecules*. 2016;82:871-877. doi:10.1016/j.ijbiomac.2015.10.024
52. Naznin R. Extraction of chitin and chitosan from shrimp (*Metapenaeus monoceros*) shell by chemical method. *Pakistan J of Biological Sciences*. 2005;8(7):1051-1054. doi:10.3923/pjbs.2005.1051.1054
53. Puvvada YS, Vankayalapati S, Sukhavasi S. Extraction of chitin from chitosan from exoskeleton of shrimp for application in the pharmaceutical industry. *Int Curr Pharm J*. 2012;1(9):258-263. doi:10.3329/icpj.v1i9.11616
54. Polat H. *Kitin ve Kitosan biyosorbentlerinin pembe karides (parapenaeus longirostris) kabuk atıklarından sentezlenmesi karakterizasyonu ve karşılaştırmalı zehirli metal adsorpsiyon çalışmaları*. Tübitak Proje(106T111); 2008.
55. Bartnicki-Garcia S. *The Biochemical Cytology of Chitin and Chitosan Synthesis in Fungi: Elsevier*. Elsevier; 1989.
56. Trimukhe K, Varma A. A morphological study of heavy metal complexes of chitosan and crosslinked chitosans by SEM and WAXRD. *Carbohydrate Polymers*. 2008;71(4):698-702. doi:10.1016/j.carbpol.2007.07.010
57. Bingöl EB, Uran H, Bostan K, Varlik C, Sivri N, Alakavuk DU. Kitosanla muamelenin dondurulmuş karideslerin duyu ve kimyasal kalite parametreleri üzerine etkisi. *Kafkas Univ Vet Fak Derg*. Published online 2013. doi:10.9775/kvfd.2012.7902
58. Arancibia MY, López-Caballero ME, Gómez-Guillén MC, Montero P. Chitosan coatings enriched with active shrimp waste for shrimp preservation. *Food Control*. 2015;54:259-266. doi:10.1016/j.foodcont.2015.02.004
59. Imansari DR, Riyadi PH, Rianingsih L, Arifin MH. Activity of *Rhizophora* sp. Extracts as Antibacterial on Shrimp during Cold Storage. *Asian J Res Biol*. 2023;6(1):71-77.
60. Lian F, Mâge I, Lorentzen G, et al. Exploring the effect of inhibitors, cooking and freezing on melanosis in snow crab (*Chionoecetes opilio*) clusters. *Food Control*. 2018;92:255-266. doi:10.1016/j.foodcont.2018.04.055
61. Martínez-Alvarez O, Elvira López-Caballero M, Montero P, del Carmen Gómez-Guillén M. The effect of different melanosis-inhibiting blends on the quality of frozen deep-water rose shrimp (*Parapenaeus longirostris*). *Food Control*. 2020;109:106889. doi:10.1016/j.foodcont.2019.106889



62. Nirmal NP, Benjakul S. Retardation of quality changes of Pacific white shrimp by green tea extract treatment and modified atmosphere packaging during refrigerated storage. *International Journal of Food Microbiology*. 2011;149(3):247-253. [doi:10.1016/j.ijfoodmicro.2011.07.002](https://doi.org/10.1016/j.ijfoodmicro.2011.07.002)
63. Gómez-Guillén MC, Martínez-Alvarez Ó, Llamas A, Montero P. Melanosis inhibition and SO<sub>2</sub> residual levels in shrimps (*Parapenaeus longirostris*) after different sulfite-based treatments. *J Sci Food Agric*. 2005;85(7):1143-1148. [doi:10.1002/jsfa.1990](https://doi.org/10.1002/jsfa.1990)
64. López-Caballero ME, Martínez-Álvarez O, Gómez-Guillén MC, Montero P. Several melanosis-inhibiting formulas to enhance the quality of deepwater pink shrimp (*Parapenaeus longirostris*). *Innovative Food Science & Emerging Technologies*. 2019;51:91-99. [doi:10.1016/j.ifset.2018.07.008](https://doi.org/10.1016/j.ifset.2018.07.008)
65. Sae-leaw T, Benjakul S, Vongkamjan K. Retardation of melanosis and quality loss of pre-cooked Pacific white shrimp using epigallocatechin gallate with the aid of ultrasound. *Food Control*. 2018;84:75-82. [doi:10.1016/j.foodcont.2017.07.029](https://doi.org/10.1016/j.foodcont.2017.07.029)